Journal of Geology & Exploration
Vol. 3, No. 1, June 2024 : 1 – 12
E-ISSN 2963-2869

Identification of Geothermal Prospect Zones in Bittuang Area Based on Remote Sensing and Geochemical Data

Ali Imran
Instutut Teknologi dan Bisnis Arung Palakka, Bone, South Sulawesi, Indonesia
Correspondence e-mail: imranawaru@gmail.com

ABSTRACTS

The research location is in the Bittuang area located in Tana Toraja Regency, South Sulawesi, Indonesia. The high level of risk of geothermal drilling at the exploration stage requires integrated geological and geochemical analysis. The integrated analysis is poured into the geothermal system conceptual hypothesis model used to identify geothermal prospect zones. This study focuses on Remote Sensing and Geochemistry methods. To identify the existence of geological structures and lithological interpretation as well as surface manifestations, Remote Sensing is used. Based on the results of Remote Sensing interpretation, the research area consists of 13 rock units of Tertiary to Quaternary age with geological structures in the form of normal faults and horizontal faults that are relatively north-northwest-southeast east and southwest-northeast. The manifestations present on the surface consist of traces of fumaroles and hot springs. The hot springs consist of the chloride type in the centre of the site and the bicarbonate type in the south of the study area. The results of geothermometer calculations of geochemical data obtained a subsurface temperature of 176 -198 °C, which is categorized as a moderate to high temperature geothermal system. The geothermal conceptual model built based on the integration of geological and geochemical data shows that the geothermal system is influenced by volcanic activity and controlled by the structure of the research area. The area of the prospect is about 4 km^2 with the up-flow area in the middle of the area while the outflow is in the South.

https://doi.org/ 10.58227/jge.v3i1.136

ARTICLE INFO

Article History:
Received 12 Feb 2024
Revised 13 Feb 2024
Accepted 03 Jun 2024
Available 30 Jun 2024

Keyword:
Geothermal, Subsurface, Structural Geology, Reservoir, Remote Sensing, Geochemical

INTRODUCTION

Indonesia as one of the countries of the ring of fire is proven by the development of the geothermal industry today. The existence of geothermal potential in an area can be described in the conceptual model of the geothermal system which is closely related to the delineation of prospect zones in geothermal areas. The main factor in delineating the prospect zone is an area that has high temperature and permeability. The temperature distribution has a correlation with the distribution of resistivity below the surface (Ussher, 2000). According to Caldwell (1986) there is a relationship between reservoir fluids, resistivity, porosity, and temperature. According to Grindley and Browne (1975), structural and hydrological factors greatly affect the condition of geothermal systems dominated by water such as the Broadlands field in New Zealand. Remote Sensing is used in Japan to identify the straightness of structures (Yamaguchi, Hase and Ogawa 1992).

The resiliency model is related to faults, fluid flow (hydrology), temperature and change zones (alterations) in the Coso geothermal field (Newman, 2008). By knowing the subsurface conditions, a geothermal conceptual hypothesis model can be built. The reservoir temperature and the potential area of the geothermal region can be used to calculate the potential. Given the importance of the analysis of the geothermal system conceptual hypothesis model that will be used as a reference in identifying geothermal prospect zones at the exploration stage.

Journal of Geology & Exploration
Vol. 3, No. 1, June 2024 : 1 – 12
E-ISSN 2963-2869

METHODS

Delineating the geothermal prospect zone begins by conducting an interpretation analysis of Landsat 7 imagery to identify the lithology and surface structure of the study area. To identify the presence of low resistivity zones and reservoir areas. Then geochemical data as supporting data will be integrated to create a conceptual hypothesis model in delineating geothermal prospect zones.

Tectonic setting was analysed to determine the tectonic conditions that were related to the conditions of the research area. Meanwhile, regional geology which includes aspects of geomorphology, stratigraphy and geological structure to be used as a reference and linked in interpreting and analysing data in research areas related to geothermal heat. Landsat 7+ETM image as a reference in interpreting and analysing the surface geological conditions of the research area.

The analysis of Landsat 7 imagery in the research area was carried out in the following order:

a. Analysed the hue in the satellite image by looking at the color difference produced by the satellite imagery.
b. Analysed the texture by paying attention to the relationship between the hues of the image.
c. Analysis of the shape contained in the aerial photograph because some rocks can form certain patterns such as lava and pyroclastic and fluvial.
d. Analysis of patterns that indicate topographic shapes, especially the straightness contained in the satellite image, which indicates the geological structure.

Geological data is used to analyse the geomorphological, stratigraphic and geological structure aspects of the research area. Meanwhile, geochemical data is used to determine the type of water, type of fluid and subsurface temperature of the research area.

RESULTS AND DISCUSSION

Sulawesi is located at the confluence of the Eurasian large plate, the Pacific plate, as well as several smaller plates (the Philippine plate) which causes its tectonic conditions to be very complex. Collections of rocks from archipelago arcs, mudstones, ophiolites, and blocks from microcontinents are carried along with subduction, collision, and other tectonic processes (Van Leeuwen, 1994). Based on the lithocholic state, Sulawesi is divided into three mandalas, namely: the west mandala as a magmatic path which is the eastern tip of the Sunda Exposure. The central mandala is a malihan rock that is topped by a bancuh rock as part of the Australian block, and the eastern mandala is an ophiolite which is a segment of the oceanic crust and sedimentary rocks of Triassic-Miocene age.

The central part of West Sulawesi Mandala is a developing research area with horizontal faults in the northwest-southeast direction and upward faults in the northeast-southwest direction. The horizontal faults in question are the Malimbo Horizontal Fault in the northern part of the research area, the West Walanae Fault in the southwest of the research area and the most dominant ascending fault is the Makale Ascending Fault in the southwest and the Anjak Latimojong Fault in the southwest of the research area (Djurt and Sudjatmiko, 1974). Van Leeuwen (1994) mentioned that the western mandala as a magmatic arc can be distinguished into two, namely the northern and western parts. The northern part extends from Buol to around Manado, and the western part from Buol to around Makassar. The northern rocks are rhodacidic to andesite, formed in the Miocene-Recess with basaltic bedrock formed in the Eocene-Oligocene. The western magmatic arc has more continental constituent rocks consisting of volcanic rocks and sedimentary rocks of Mesozoic-Quaternary age and Cretaceous age majestic rocks. The rock was broken through by granitoids composed mainly granodioritic - granitic in the form of batolite, stock, and hack.

The northern and southern arms are formed by a geological unit called the West Sulawesi mandala. Similarly, the eastern arm and the southeast arm are one geological unit referred to as the mandala of East Sulawesi. The two Sulawesi arcs are joined together in the Central Sulawesi area but are clearly separated to the south by Bone Bay and north by Tomini Bay. The two bays are more than thousands of meters deep, the size of the area of the two bays is filled with sedimentary rocks with a thickness of about thousands of meters and seems to have oceanic bedrock in the deepest part of the two bays. Sartono, et al. (1991) said that the movement of the Banggai Micro continent to the west which was previously torn off from the northern edge of the Australian Continent in Irian Jaya – Papua New Guinea through the Sorong fault began to occur at the end of the Lower Miocene. The Banggai Micro Continent which is at the forefront collided with the Sunda arc which resulted in the obduction of mafic-ultramafic rocks and mixed with tectonic melange and caused the occurrence of various Quaternary age coastal steps, the elevation of which reached several hundred meters. The collision between the Banggai Micro continent and the non-volcanic arc above squeezed and narrowed the basin in front of the Sunda Arc until it caused the formation of the central ridge of Sulawesi which was partially covered by Lake Poso and Bone Bay and Tomini Bay.

Journal of Geology & Exploration
Vol. 3, No. 1, June 2024 : 1 – 12
E-ISSN 2963-2869

Based on the interpretation of images from Remote Sensing using Landsat 7 satellite images combined with the results of geological investigations in the field by the PSDG Geological Survey Team (2009), the rocks in the study area can be grouped into 13 rock units, consisting of one malihan rock unit, one sedimentary rock unit and eleven volcanic rock units. The sequence of rock units or stratigraphy from old to young (Figure 1) is Malihan rock units (Kbm), Ruppu Sandstone (Rbp), Mount Ruppu Pyroclastic (Rpl), Mount Rantebombong Pyroclastic (Rp4), Mount Panusuk Pyroclastic (Ppl), Mount Karua Pyroclastic (Kpl), Mount Ruppu Pyroclastic Fluvio (Rf1), Mount Karua Pyroclastic Fluvio (Kf1), Mount Karua Fan Fluvio (Kff), Mount Malibu Lava (Ml1), Mount Karua Lava (Kl4), Mount Karua Lava (Kl3), Mount Karua Lava (Kl1).

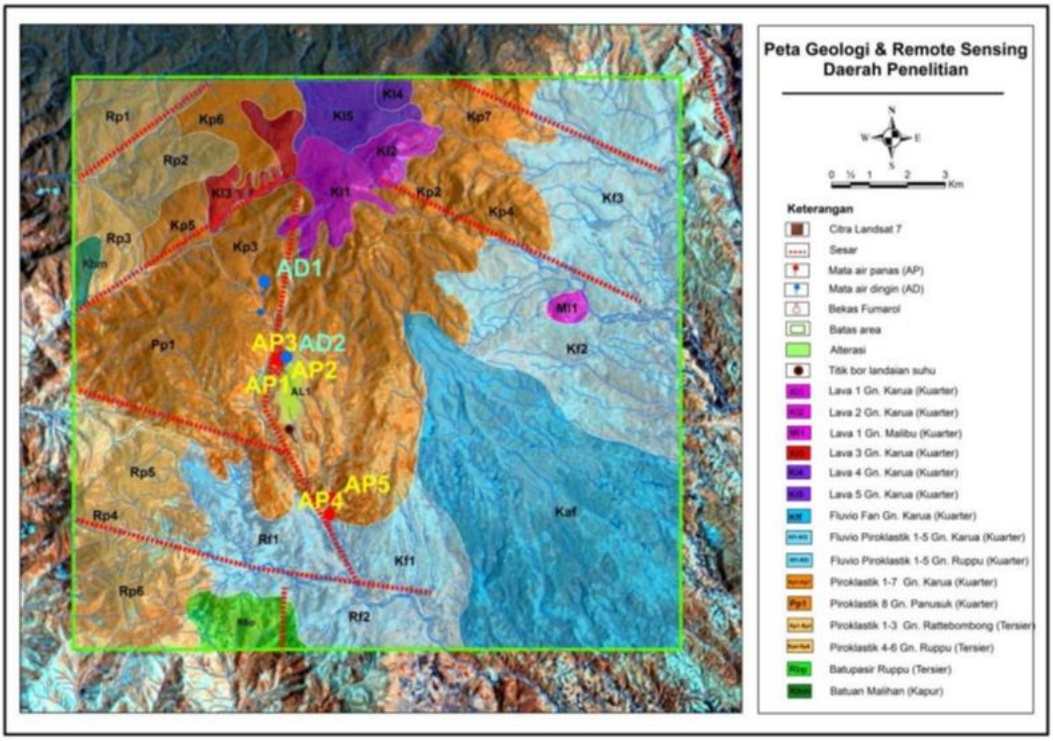

Figure 1. Geological Maps & Remote Sensing of Research Areas

Based on the texture and hue in Remote Sensing, the research area is divided into three parts of lithology, namely: a. Lava in the Landsat 7 image, the interpretation of the existence of lava in the research area is characterized by a dark and homogeneous hue and a smoother appearance which indicates that the material is solid and has not experienced surface erosion. In addition, lava flows are characterized by textured edges that get smaller and smaller or disappear as they go to the end. The interpretation of the existence of lava in the study area can be seen in Figure 1, namely the codes Kl1, Kl2, Kl3, Kl4 and Ml1. b. Pyroclastic in the Landsat 7 image, the interpretation of the existence of pyroclastic in the study area is characterized by almost dark and slightly bright hues and semi-homogeneous. The texture looks rougher than lava and is not smooth (flat) which indicates that the material is not so solid and has undergone surface erosion which is marked by the presence of a pattern or channel on the surface of the image. In addition, pyroclastic is also characterized by a texture that is relatively radial which indicates the direction of the flow that has been eroded by water. The interpretation of the existence of pyroclastic in the research area can be seen in Figure 1, namely the codes Rbp, Rpl, Rp4, Pp1 and Kpl. c. Volcanic Fluvio in the Landsat 7 image, the interpretation of the existence of volcanic fluvio in the study area is that it has characteristics such as bright and heterogeneous hues. The texture looks mixed and far from the source of the eruption, indicating that the material is fine material derived from pyroclastic falls or lava that has been transported to lower areas. The research area is divided into two, namely pyroclastic fluvio and fan fluvio. Pyroclastic fluvio comes from pyroclastic or transported lava falls, while fan fluvio comes from pyroclastic or lava materials that are transported and deposited whose morphology forms like a fan. The interpretation of the existence of pyroclastic fluvio in the study area can be seen in Figure 1, namely the Kfl code and the fan fluvio with the Kff code.

Journal of Geology & Exploration
Vol. 3, No. 1, June 2024 : 1 – 12
E-ISSN 2963-2869

The interpretation of surface manifestations in the research area is focused on areas close to the top of the mountain. Texture and hue are the basic reference in the interpretation of images such as images with the appearance of homogeneous and dominant textures and the appearance of subtle hues. In Figure 2, the red circle line is estimated to be a surface manifestation that can be either a surface alteration material or a fine material on the surface.

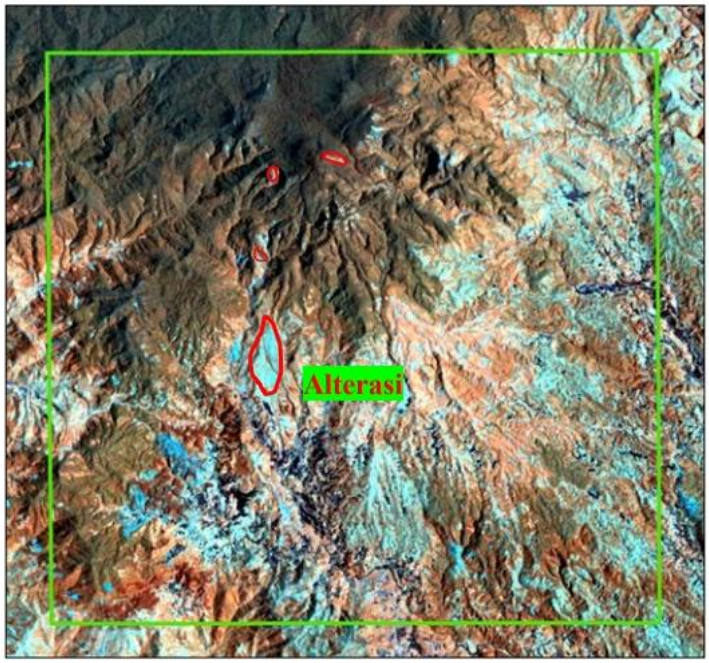

Figure 2. Interpretation of surface manifestations based on Remote Sensing.

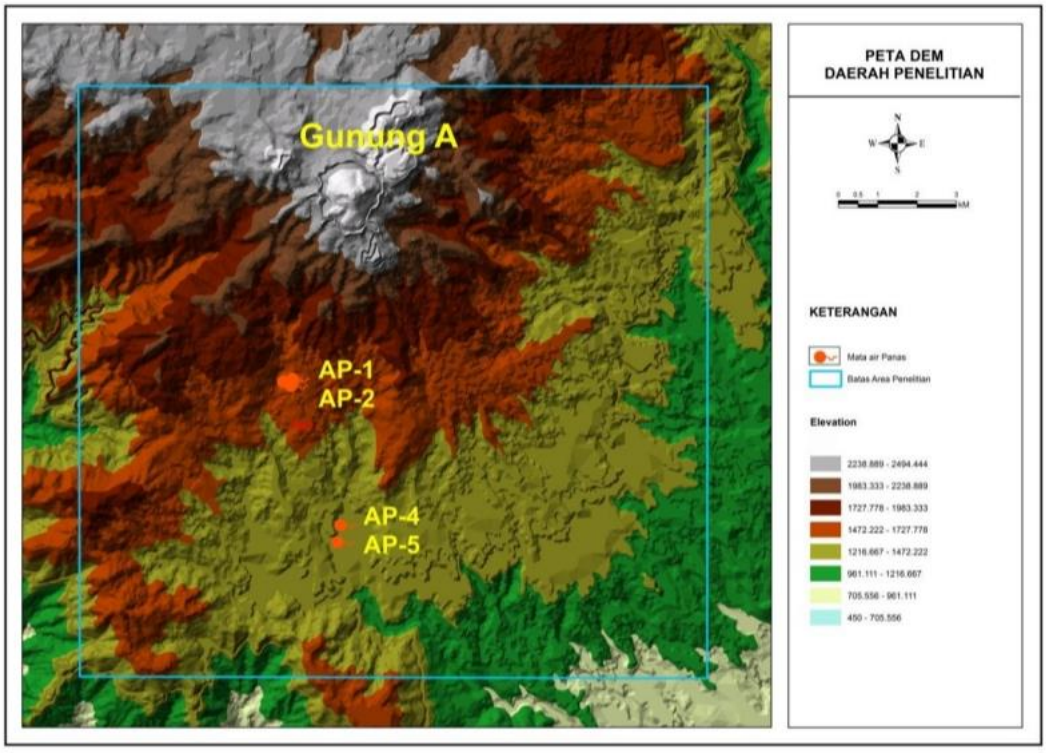

Figure 3. Digital Elevation Model (DEM) map of the research area.

Journal of Geology & Exploration
Vol. 3, No. 1, June 2024 : 1 – 12
E-ISSN 2963-2869

Figure 4. Geomorphological photo of the mountains of the research area, taken from the south.

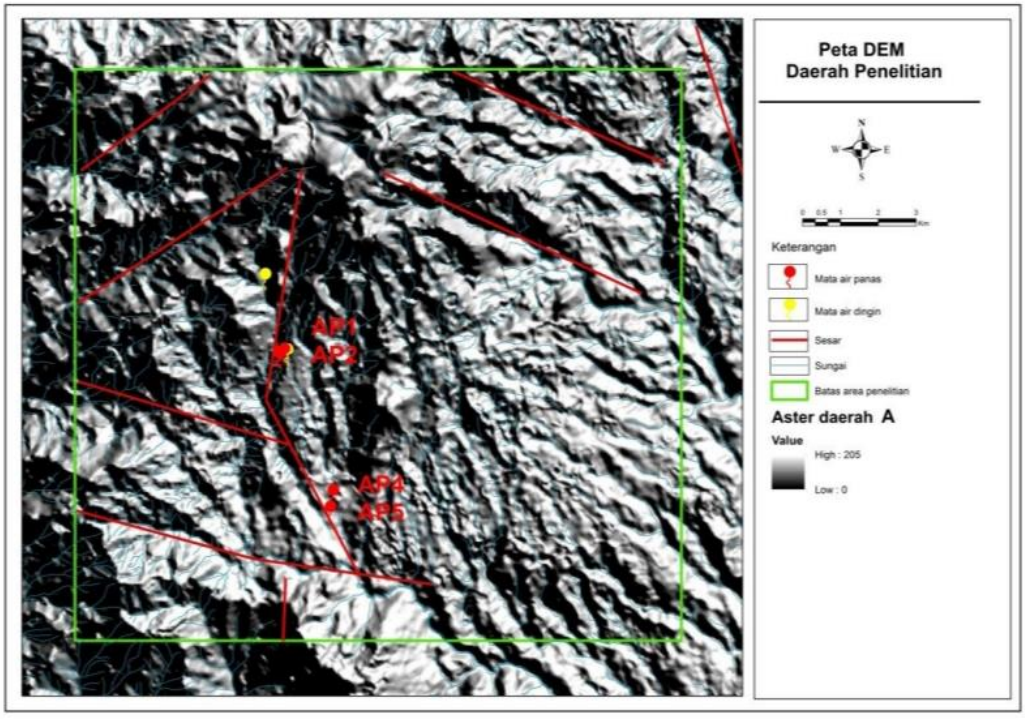

Figure 5. DEM map of the research area

Analysis on the DEM (Digital Elevation Model) and ASTER maps shows that the geological structure in the investigation area is dominated by geological structures in the form of faults (Figure 5). These fault structures are generally northwest-southeast, north-south and northeast-southwest. These normal faults are estimated to be the medium for the exit of a few hot springs at the investigation site. Based on observations in the field, it was found that it was not systematic (Figure 6) on the tufa outcrop.

Journal of Geology & Exploration
Vol. 3, No. 1, June 2024 : 1 – 12
E-ISSN 2963-2869

Figure 6. Photo of Kekar on the tufa outcrop, taken from the south.

Based on the processing of sturdy data using fan and stereonet fan diagrams (Figure 7), the direction of maximum main stress (σ1) was obtained, which is about N 350o E, relatively north-northwest-southeasteast.

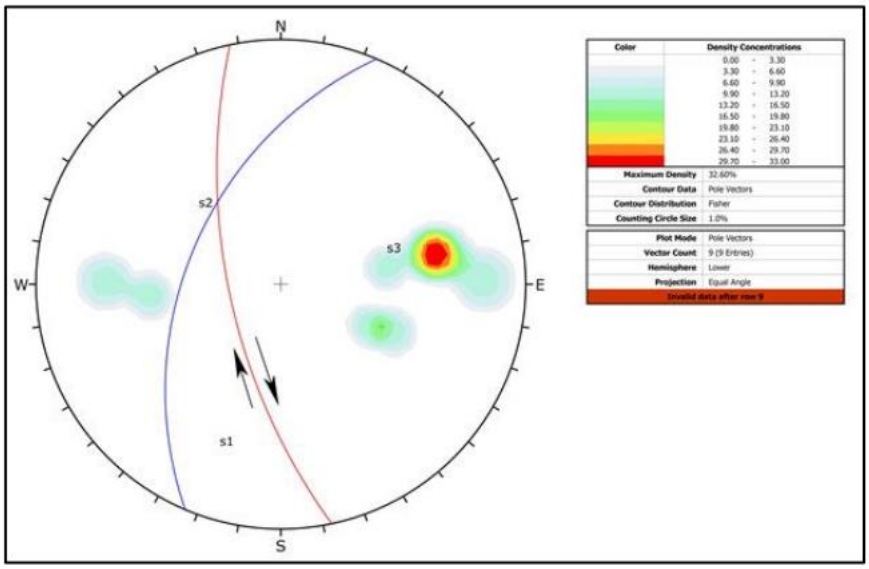

Figure 7. Robust data processing stereonet to determine the direction of the main stress.

Based on the structural data from the investigation in the field, the analysis of the DEM (Digital Elevation Model) map and topographic map, as well as the appearance of spring alignment as a symptom of the structure on the surface, the straightness of the valley and ridge, and the burly crust, the research area has a fault structure, namely: a. Normal faults are almost north-northwest-southeast (local faults) that control the occurrence of geothermal manifestations in the hot springs AP-1, AP-2, AP-3, AP-4 and AP-5. The determination of this fault is based on field data where a vertical σ1 is obtained, a normal fault will be formed (Anderson, 1951 in Davis and Reynold, 2011). b. Horizontal faults are in the southwest-northeast and northwest-southeast directions which cut and cause shifts in previously formed rocks and structures. The determination of this fault is based on the topographic analysis of the research area,

Alterations in the detailed research area are in the form of the dominance of argillic clay around the rim of the Parakasak caldera and aseupan, as well as argillic clay – prophilitic chlorite around the north of Parakasak, while the top tends to be silica-clay alteration. Alteration in the Aseupan area is

Journal of Geology & Exploration
Vol. 3, No. 1, June 2024 : 1 – 12
E-ISSN 2963-2869

likely to be a fossil alteration, which is evidenced by the widespread distribution of 7rgillic clay in the form of kaoline-smectite and has been eroded along the direction of the collapse rim of the Aseupan caldera. In addition, traces of solfatara were also found, which are indicated by the presence of sulphur (partly in the form of crystals) by filling in fracture or breechation structures.
The emergence of hot springs in the north of Parakasak is indicated by the influence of rock contact structures, which can be seen from the bubble spring trend pattern that follows the contact pattern of Parakasak rocks, which are relatively southwest – northeast.

Geochemistry

Surface Manifestation Based on data sourced from PSDG Bandung (2009), the surface manifestation data in the research area include the following:
a. In the central part of the research area consists of AP-1, AP-2 and AP-3 hot springs and the presence of gas from former fumaroles because the gas blowing has a pressure that is not too large. In the former fumarole, there is a smell of H2S gas, there is sulfur sublimation with the highest temperature of 96.7o C. In addition, there are also cold springs, namely AD-1 and AD-2.
b. In the central part of the location, altered rocks (alterations) were also found scattered locally to the north of the AP-1 and AP-2 hot spring manifestation groups in the area that showed a dead solfatara field, The field area was indicated by the discovery of sulfur deposits and altered rocks.
c. In the southern part of the research area consisting of AP-4 and AP-5 hot springs around the rice field area, there is silica sintering. d. Drill a temperature ramp at a depth of 363 meters with a temperature of 44o C.

Water Chemical Analysis Based on the results of the PSDG integrated investigation in 2009, the symptoms of surface geothermal appearance are characterized by the appearance of several hot springs, which consist of hot springs AP-1, AP-2, AP-3, AP-4 and AP-5 while cold springs consist of AD-1 and AD-2. In the hot springs in the middle of the research site, there are three hot springs, namely: AP-1, AP-2 and AP-3 hot springs. The AP-1 and AP-2 hot springs are located at an elevation of 1592 meters while the AP-3 hot springs are located at an elevation of 1680 meters. In the hot springs AP-1 and AP-2 it looks clear, salty and there is sintered silica, while in the hot springs AP-3 it is clear, sour and the bottom of the water flow is yellow. The three hot springs AP1, AP2 and AP3 are located around fumaroles whose gas pressure is not too great. In the hot springs in the southern part there are two hot springs, namely: AP-4 and AP-5 hot springs. The AP-4 hot spring is located at an elevation of 1256 meters while the AP-5 hot spring is located at an elevation of 1269 meters. In AP-4 hot springs it looks clear, sour and there is iron oxide, while in AP-5 hot springs it is clear in color, sour and there is iron oxide. AP-4 and AP-5 hot springs are located around rice fields and small river banks

Figure 8. AP-1 hot springs

Journal of Geology & Exploration
Vol. 3, No. 1, June 2024 : 1 – 12
E-ISSN 2963-2869

Figure 9. AP-4 hot springs

Table 1. Data from the Chemical Analysis of Surface Manifestation Water (PSDG Bandung, 2009)

Code	AP-1	AP-2	AP-3	AP-4	AP-5	AD-1	AD-2
Elev (m)	1592	1592	1680	1256	1269	1767	1644
T(°C) water	96.70	90.50	48.10	37.60	39.80	17.20	18.30
T(°C) air	22.50	21.60	18.80	22.10	201.0	19.10	22.90
Ph	8.40	7.76	5.40	6.28	5.97	4.20	7.50
EC (µS/cm)	9700.00	8400.00	222.00	2630.00	1241.00	320.00	69.00
SiO2 (mg/L)	179.70	153.04	114.85	159.86	170.25	94.60	56.98
Al	0.16	0.10	0.00	0.00	0.00	4.49	0.00
Fe	0.09	0.07	0.06	4.73	3.09	0.50	0.01
Ca	5.57	12.08	9.28	190.20	119.34	30.51	4.13
Mg	1,50	1.00	0.07	105.60	45.90	1.40	0.33
Na	1848.00	1504.00	50.80	210.96	65.68	9.80	5.00
K	92.60	68.50	13.61	13.30	4.56	1.00	0.50
Li	10.40	7.90	0.04	1.20	0.48	0.02	0.01
Axle	8.00	4.00	0.10	0.00	0.00	0.00	0.00
NH4	0.00	0.00	0.00	0.00	0.00	0.00	0.00
B	85.18	76.86	0.76	9.21	0.93	0.00	0.00
F	1.00	0.50	0.30	0.50	0.50	0.50	0.00
Cl	2459.71	2144.00	80.13	376.40	105.11	2.00	0.50
SO4	378.58	4.00	4.00	60.33	4.00	140.67	15.00
HCO3	223.00	49.36	49.35	998.25	592.94	0.00	7.39
CO3	0.00	0.00	0.00	0.00	0.00	0.00	0.00
Meq Cat	85.00	69.18	3.04	28.12	12.94	2.62	0.47
Meqan	80.97	68.90	3.17	28.26	12.79	3.01	0.45
% IB	2.43	0.20	-2.07	-0.24	0.58	-6.99	1.97

Based on geochemical analysis on the surface manifestations of the research area, it can be used as a reference in interpreting geochemical processes under the surface. The geochemical process under the surface can be determined by using the results of chemical analysis such as water type, fluid origin, reservoir temperature and geochemical anomalies in the investigation area. From the data from the analysis of water chemistry from surface manifestations, it is included in a triangular diagram (ternary diagram) popularized by Giggenbach (1988, 1991) to estimate the origin of fluids based on the chemical equilibrium of fluids in geothermal reservoirs. Triangle diagrams of major anions and cations that include chloride (Cl) – sulphate (SO4) – bicarbonate (HCO3) as well as Na-K-CaMg are mostly relevant for use in evaluating fluids in geothermal prospect regions.

Based on geochemical analysis on the surface manifestations of the research area, it can be used as a reference in interpreting geochemical processes under the surface. The geochemical process under the surface can be determined by using the results of chemical analysis such as water type, fluid origin, reservoir temperature and geochemical anomalies in the investigation area. From the data from the analysis of water chemistry from surface manifestations, it is included in a triangular diagram

Journal of Geology & Exploration
Vol. 3, No. 1, June 2024 : 1 – 12
E-ISSN 2963-2869

(ternary diagram) popularized by Giggenbach (1988, 1991) to estimate the origin of fluids based on the chemical equilibrium of fluids in geothermal reservoirs. Triangle diagrams of major anions and cations that include chloride (Cl) – sulphate (SO4) – bicarbonate (HCO3) as well as Na-K-CaMg are mostly relevant for use in evaluating fluids in geothermal prospect regions.

Based on the results of the water chemistry data plot in the Ternary Diagram Cl-SO4-HCO3 (Figure 10), it shows that AP-1 and AP-2 hot water belong to the sodium chloride type that reflects the reservoir fluid. Meanwhile, AP-4 and AP-5 hot water contain high bicarbonate which reflects more dominant meteoric water.

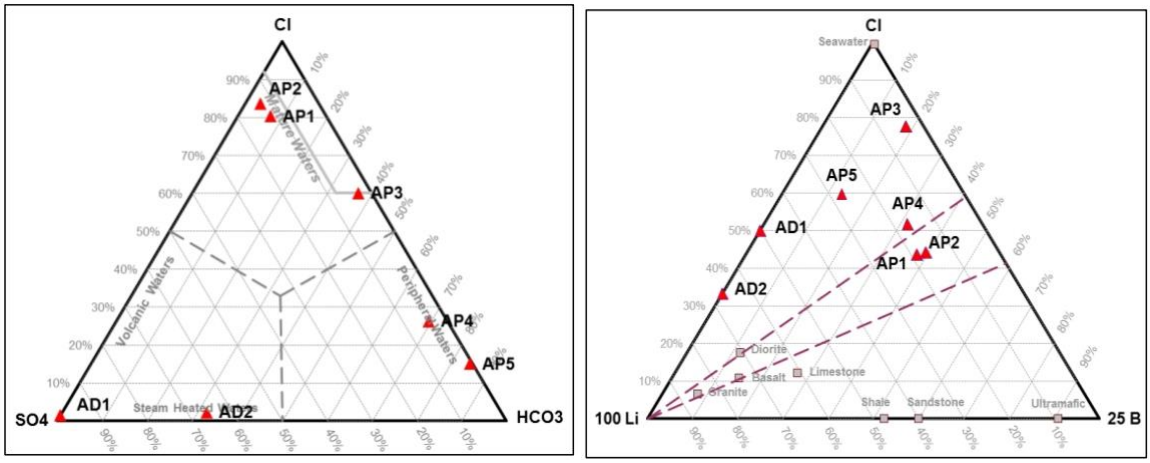

Figure 10. Ternary Diagram Cl-SO4-HCO3 and Ternary Diagram Cl-Li-B

Based on the results of the plot in the Ternary Diagram Cl-Li-B (Figure 10), it can be shown that in the AP-4 and AP-5 hot springs, the ratio of B/Cl is smaller, and the ratio of Li/Cl is smaller. A smaller Cl value indicates that the fluid has moved laterally which is thought to be more mixed with meteoric water. In the AP-1 and AP-2 hot spring groups, the ratio of B/Cl is greater, and the ratio of Li/Cl is larger. The larger Cl value indicates that the AP-1 and AP-2 hot spring samples are expected to be closer to the reservoir zone.

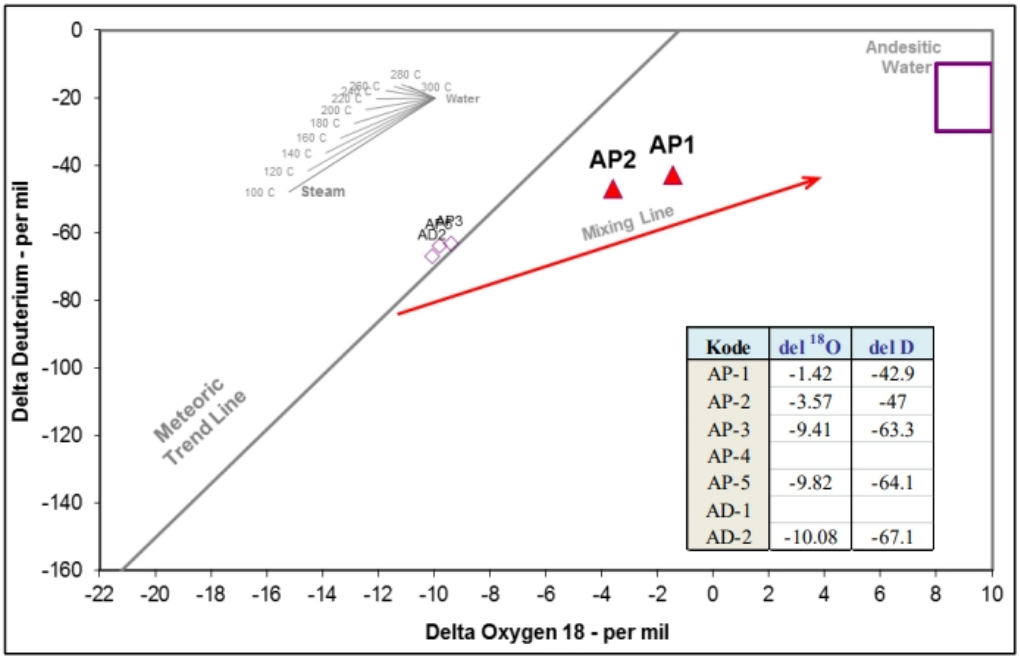

Figure 11. The relationship between the ratio of isotopes 18 O to 2H fluids.

Based on the plot results in the graph of the relationship between the isotope ratio of 18 O and 2H geothermal fluids (Figure 11), it shows that the hot springs AP-1 and AP-2 are on the mixing line

Journal of Geology & Exploration
Vol. 3, No. 1, June 2024 : 1 – 12
E-ISSN 2963-2869

where they have values that are close to the composition value of the isotope 18 O of magmatic water. From this data, it can indicate two possibilities, namely the interaction of reservoir water with meteoric water and the possibility of mixing meteoric water with magmatic water. Based on the Na-K-Mg ternary diagram (Figure 12), it is shown that the AP-1 and AP-2 hot springs derived from hot spring samples in the center of the research site are in the partial equilibrium position which can then be used for temperature estimation using a geothermometer cation. Meanwhile, in the hot springs AP-3 and AP-4 and AP-5 which came from hot spring samples in the southern part of the study site, there was a high Mg content, where in most water chemistry showed the origin of meteoric fluids or predominantly in the immature water area in the major cation plot (Na-K-Mg). For samples that are in immature water, they are usually mixed with shallow groundwater, so the results of the geothermometer calculation cannot represent the actual temperature of the reservoir fluid.

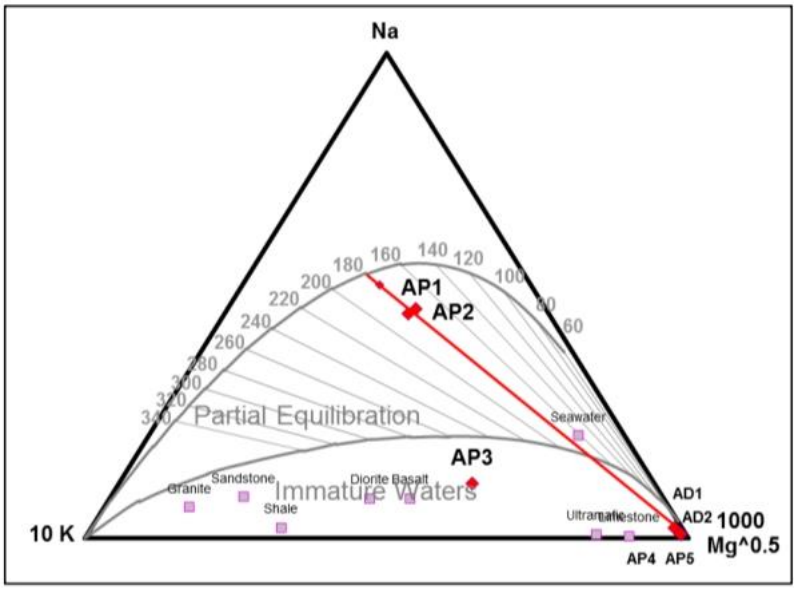

Figure 12. Reservoir temperature estimates were made using the Ternary Diagram Na-K-Mg.

Table 2. Data from the analysis of water chemical geothermometers

Sample Name	Na – K - Ca	Na – K – Fish Mg corr	Na/K Fournier 1979	Na/K Giggenbach 1988	Na/K Arnorsson 1983	K/Mg Giggenbach 1986
AP1	198	181	164	183	134	160
AP2	182	176	158	176	126	156
AP3	232	223	319	325	323	146
AP4	67	44	180	198	152	48
AP5	36	36	188	205	161	35
AD1	7	7	219	234	197	40
AD2	16	16	217	232	195	40

Based on the calculation of Na-K-Ca and Na-K-Ca geothermometers with Mg correction for AP-1 and AP-2 hot spring samples, where both show similar geothermometer values of 176 – 198o C which can be estimated as the temperature of the reservoir in the study area.

Journal of Geology & Exploration
Vol. 3, No. 1, June 2024 : 1 – 12
E-ISSN 2963-2869

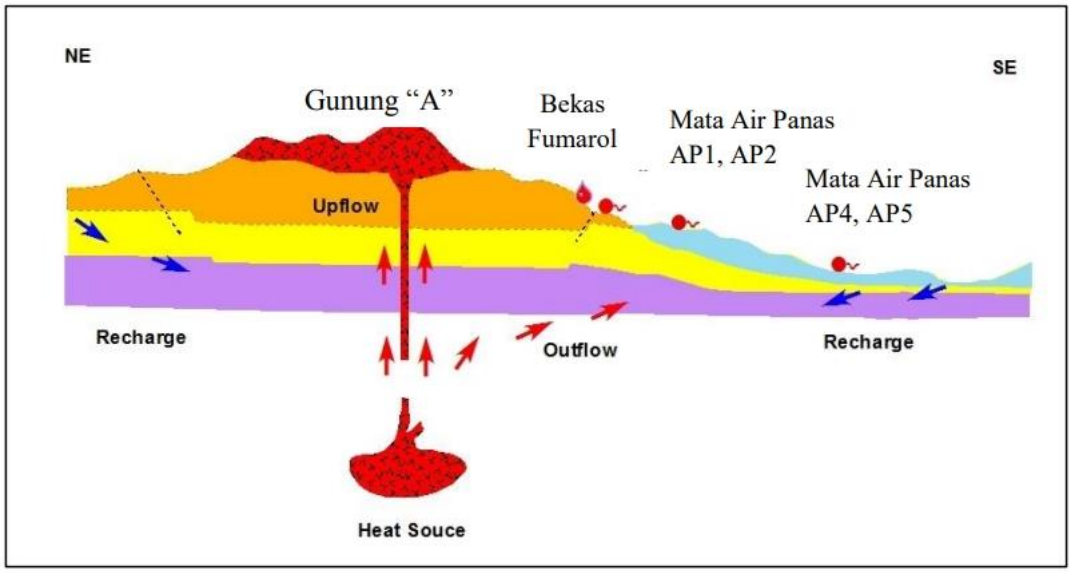

Figure 13. Geothermal hypothesis model of the Bittuang area

The geothermal system of the study area includes volcanic systems that are influenced by local geological structures in the form of horizontal faults. Based on Remote Sensing and geological data, it shows that Mount Karua produces products in the form of quaternary lava which indicates that the heat source is suspected to come from residual magma in the volcanic activity of the Mount Karua Quaternary. The tectonic activity that causes the structure to develop in the study area can be seen by the direction of the structure based on the interpretation of Remote Sensing which is relatively in the direction of North-Northwest – South-Southeast which is in the same direction as the parallel direction of the hot springs in the research area. The emergence of surface manifestations in the form of hot springs and alterations is estimated to be controlled by the North-Northwest – South-Southeast directional structure. AP-1, AP-2 and AP-3 hot springs have medium-high temperatures ranging from 48.5º C to 96.7º C, with a pH of 7.3 – 8.4. These hot springs are associated with fumarole marks, surface alterations and silica sintering. In the southern part of the study area, there are two hot springs with low temperatures located in the rice field area with a pH ranging from 5.9 to 6.2. Based on the calculation of the hot water chemical geothermometer, the reservoir temperature was around 176 - 198 ºC (moderate to high temperature system).

CONCLUSION

After conducting data processing and data modelling in an integrated manner in the form of Remote Sensing, geology, and geochemistry, the geothermal system in the research area can be concluded. The geothermal system of the Bittuang area is influenced by Quaternary volcanic activity and is controlled by the developing structure in the research area. The stratigraphy of the study area is composed of 13 rock units, namely one unit of malihan rock, one unit of sedimentary rock and eleven units of volcanic rock. Based on the results of the interpretation, the geological structure in the research area consists of a horizontal fault in the southwest-northeast direction and a normal fault in the north-northwest-southeast direction which controls the appearance of hot spring manifestations in the research area. The subsurface temperature is estimated to be around 176o - 198o C which is related to the reservoir in the geothermal system of the study area which is included in the Moderate to high temperature geothermal system. The area of the prospect is about 3 km2 with the up flow zone in the middle of the area while the outflow zone is in the south of the research area.

ACKNOWLEDGMENT

The author would like to thank the related parties who have provided support for this research.

Journal of Geology & Exploration
Vol. 3, No. 1, June 2024 : 1 – 12
E-ISSN 2963-2869

REFERENCE

Billings, M. P. (1968). Structural Geology, Second ed. Prentice of India Private Limited, New Delhi.
Bogie, I. and Mackenzie, K.M. (1998). The application of a volcanic facies models to an andesitic stratovolcano hosted geothermal system at Wayang Windu, Java, Indonesia. Proceedings of 20th NZ Geothermal Workshop, p.265-276.
Bronto, S. (2006). Volcano Facies and Their Applications. Indonesian Journal of Geology, Vol.1 No.2.
Caldwell. (1986). Resistivity Of Rocks In Geothermal Systems. Proc. 8th Geothermal Workshop. Auckland.
Cumming, W. and Mackie R. (2007). 3D MT Resistivity Imaging for Geothermal Resource Assessment and Environmental Mitigation at the Glass Mountain KGRA, California.
Daud, Y. (2008). Geological Exploration Lecture Module. Physics Study Program. University of Indonesia.
Davis, G. H., and Reynolds, S. J. (2011). Structural Geology of Rock and Regions (Third Edition). Canada: John Wiley & Sons, Inc.
Djuri and Sudjatmiko. (1974). Geological Map of the Western Majene and Palopo Sheets, Sulawesi, Sekala 1 : 250,000. P3G Bandung.
Ellis, A.J. and Mahon, W.A.J. (1977). Chemistry and geothermal systems. Academic Press, New York, 392 pp.
Fournier, R.O. (1977). Chemical geothermometers and mixing models for geothermal systems. Geothermics, Vol. 5, 41-50.
Fournier, R.O. (1979). A revised equation for the Na/K geothermometer. Geothermal Resources Council Transactions. Volume 3, 221-224.
Giggenbach, W., Goguel, R.L. (1989). Collection&analysis of geothermal and volcanic water &gas discharges. Chemistry Division, Department of Scientific & Industrial Research, Petone, New Zealand. Report CD2401.
Goff and Janik. (2000). Geothermal System. Chapter 49 In Encyclopedia Volcanoes.
Grindley, G.W. and Browne, P.E. (1975). Structural and Hydrological Factors Controlling The Permeabilities of Some Hot Water Geothermal Fileds. New Zealand Geological Survey.
Hase, H. and Miyazaki, Y. (1976). Geothermal Resources Map Aided by Remote Sensing Data. Japan.
Hersir, G. P., and Arnason, K. (2010). Resistivity of Rocks. UNU-GTP.
Hochstein, M. P., and Browne, P. R. (2000). Surface Manifestations of Geothermal Systems with Volcanic Heat Sources. In Encyclopedia of Volcanoes (p. 835). Academic Press.
Lillesand, T. M., and Kiefer, R.W. (1979). Remote Sensing & Image Interpretation (translation), third edition, John Wiley & Sons.
Nicholson, K. (1993). Geothermal fluids: chemistry and exploration techniques, Springer-Verlag Berlin, Heidelberg New York.
Peng, F. (2013). Towards Application of Remote Sensing Technology in Geothermal Prospecting in Xilingol in Eastern Inner Mongolia, NE
Pinael, P. (2011). Geothermal Potential of Bittuang. http://pilarge04.blogspot.com/
Powell and Cumming. (2000). Liquid & Gas Analysis Excel Spreadsheets. Stanford University's Geothermal Program, California.
Center for Geological Resources (PSDG). (2009). Integrated Survey of Geology & Geochemistry of Bittuang Area. Bandung.
Ratman and Atmawinata,. (1993). Geological Map of Mamuju Sheet, SulawesiSekala 1 : 250,000. P3G Bandung.
Sartono, S. (1991). East Arm Sulawesi ; Banggai Microplate - Sunda Subduction Zone Collision, Indonesia.
Sewell, S.M. (2012). Integrated MT And Natural State Temperature Interpretation For A Conceptual Model Supporting Reservoir Numerical Modelling And Well Targeting At The Rotokawa Geothermal Field, New Zealand. Workshop on Geothermal Reservoir Engineering, Stanford University, California.
Sompotan, A.F. (2012). Geological Structure of Sulawesi. ITB Bandung.
Taylor and Francis. (2007). Series in Remote Sensing Applications.